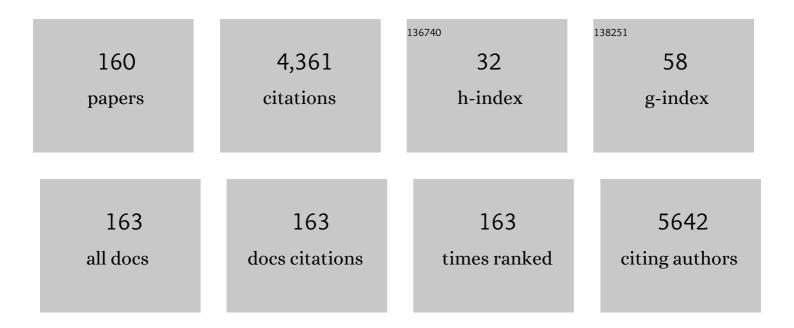


List of Publications by Year in descending order

Source: https://exaly.com/author-pdf/3697991/publications.pdf Version: 2024-02-01



Huu Ou

#	Article	IF	CITATIONS
1	CQDs as emerging trends for future prospect in enhancement of photocatalytic activity. Carbon Letters, 2022, 32, 81-97.	3.3	19
2	Metastable FeCN ₂ @nitrogen-doped carbon with high pseudocapacitance as an anode material for sodium ion batteries. Nanoscale, 2022, 14, 780-789.	2.8	7
3	A CdS/MnS p–n heterojunction with a directional carrier diffusion path for efficient photocatalytic H ₂ production. Inorganic Chemistry Frontiers, 2022, 9, 1100-1106.	3.0	15
4	A three-dimensional coral-like Zn,O-codoped Ni3S2 electrocatalyst for efficient overall water splitting at a large current density. Sustainable Energy and Fuels, 2022, 6, 466-473.	2.5	0
5	Molybdenum and cobalt co-doped VC nanoparticles encapsulated in nanocarbon as efficient electrocatalysts for the hydrogen evolution reaction. Inorganic Chemistry Frontiers, 2022, 9, 870-878.	3.0	13
6	Metal–Molecule–Metal Junctions on Self-Assembled Monolayers Made with Selective Electroless Deposition. ACS Applied Materials & Interfaces, 2022, 14, 1609-1614.	4.0	4
7	<i>In situ</i> construction of superhydrophilic crystalline Ni ₃ S ₂ @amorphous VO _{<i>x</i>} heterostructure nanorod arrays for the hydrogen evolution reaction with industry-compatible current density. Dalton Transactions, 2022, 51, 7234-7240.	1.6	5
8	Controlled phase and crystallinity of FeNCN/NC dominating sodium storage performance. Dalton Transactions, 2022, , .	1.6	2
9	MoS ₂ -Modified CdS Hexagonal Pyramid To Form a New Photogenerated Carrier Migration Path with Highly Efficient Photocatalytic H ₂ Performance. Journal of Physical Chemistry C, 2022, 126, 9027-9033.	1.5	6
10	The Semicoherent Interface and Vacancy Engineering for Constructing Ni(Co)Se ₂ @Co(Ni)Se ₂ Heterojunction as Ultrahighâ€Rate Batteryâ€Type Supercapacitor Cathode. Advanced Functional Materials, 2022, 32, .	7.8	57
11	Mechanical properties of large-sized thin architectural ceramic plate enhanced by alumina fibres and in situ mullite whiskers. Processing and Application of Ceramics, 2022, 16, 183-190.	0.4	3
12	Tuning the electronic communication of the Ru–O bond in ultrafine Ru nanoparticles to boost the alkaline electrocatalytic hydrogen production activity at large current density. Inorganic Chemistry Frontiers, 2022, 9, 4151-4159.	3.0	9
13	Graft PEI ultra-antiwear nanolayer onto carbon spheres as lubricant additives for tribological enhancement. Tribology International, 2021, 153, 106652.	3.0	15
14	Ultrafine VN nanoparticles confined in Co@N-doped carbon nanotubes for boosted hydrogen evolution reaction. Journal of Alloys and Compounds, 2021, 853, 157257.	2.8	22
15	Regulation of hydrophilicity/hydrophobicity of aluminosilicate zeolites: a review. Critical Reviews in Solid State and Materials Sciences, 2021, 46, 330-348.	6.8	31
16	Defect-rich bimetallic yolk–shell metal-cyanide frameworks as efficient electrocatalysts for oxygen evolution reactions. Journal of Materials Chemistry A, 2021, 9, 2135-2144.	5.2	20
17	Sodium citrateâ€assisted synthesis of <scp>nanoâ€manganese</scp> oxide on carbon fiber for enhancing the mechanical and frictional performances of carbon fiberâ€reinforced resin matrix composites. Journal of Applied Polymer Science, 2021, 138, 50322.	1.3	3
18	Controllable synthesis of SnS2 nanoflakes as high-performance anode for lithium-ion batteries. Journal of Materials Science: Materials in Electronics, 2021, 32, 191-203.	1.1	5

#	Article	IF	CITATIONS
19	A thick titanium dioxide layer formed by Co-doping on a carbon surface promotes the polysulfide-adsorption ability in Li–S batteries. Sustainable Energy and Fuels, 2021, 5, 4153-4160.	2.5	1
20	Construction of Ge/C nanospheres composite as highly efficient anode for lithium-ion batteries. Journal of Materials Science: Materials in Electronics, 2021, 32, 6398-6407.	1.1	2
21	Cobalt-doped Vanadium Pentoxide Microflowers as Superior Cathode for Lithium-Ion Battery. Jom, 2021, 73, 808-814.	0.9	5
22	Silanization integrating TiO ₂ nanorods-carbon fiber for improving mechanical and wear-resisting behaviors of phenolic composite. Journal of Composite Materials, 2021, 55, 3191-3202.	1.2	1
23	From Hexagonal to Monoclinic: Engineering Crystalline Phase to Boost the Intrinsic Catalytic Activity of Tungsten Oxides for the Hydrogen Evolution Reaction. ACS Sustainable Chemistry and Engineering, 2021, 9, 5642-5650.	3.2	23
24	Development and Preliminary Application of Multiplex Loop-Mediated Isothermal Amplification Coupled With Lateral Flow Biosensor for Detection of Mycobacterium tuberculosis Complex. Frontiers in Cellular and Infection Microbiology, 2021, 11, 666492.	1.8	7
25	Realizing Fast Charge Diffusion in Oriented Iron Carbodiimide Structure for High-Rate Sodium-Ion Storage Performance. ACS Nano, 2021, 15, 6410-6419.	7.3	41
26	Tailoring FeP with a Hollow Urchin Architecture for High-Performance Li–S Batteries. ACS Sustainable Chemistry and Engineering, 2021, 9, 5315-5321.	3.2	22
27	Chemical Heterointerface Engineering on Hybrid Electrode Materials for Electrochemical Energy Storage. Small Methods, 2021, 5, e2100444.	4.6	62
28	Electromagnetic wave absorption properties of N-PyC/Ti3C2Tx hybrids. Journal of Materials Science: Materials in Electronics, 2021, 32, 26105-26115.	1.1	3
29	Latamoxef for Neonates With Early-Onset Neonatal Sepsis: A Study Protocol for a Randomized Controlled Trial. Frontiers in Pharmacology, 2021, 12, 635517.	1.6	3
30	Interfacial chemical bond and internal electric field modulated Z-scheme Sv-ZnIn2S4/MoSe2 photocatalyst for efficient hydrogen evolution. Nature Communications, 2021, 12, 4112.	5.8	421
31	Rational Design of Vanadium-Modulated Ni ₃ Se ₂ Nanorod@Nanosheet Arrays as a Bifunctional Electrocatalyst for Overall Water Splitting. ACS Sustainable Chemistry and Engineering, 2021, 9, 12005-12016.	3.2	38
32	Population pharmacokinetics-pharmacodynamics of ceftazidime in neonates and young infants: Dosing optimization for neonatal sepsis. European Journal of Pharmaceutical Sciences, 2021, 163, 105868.	1.9	5
33	Tuberculosis infection screening in children with close contact: a hospital-based study. BMC Infectious Diseases, 2021, 21, 815.	1.3	4
34	Vanadium -mediated ultrafine Co/Co ₉ S ₈ nanoparticles anchored on Co–N-doped porous carbon enable efficient hydrogen evolution and oxygen reduction reactions. Nanoscale, 2021, 13, 16277-16287.	2.8	11
35	Inducing [100]-orientated plate-like α-MoO3 to achieve regularly exfoliated layer structure enhancing Li storage performance. Journal of Materials Science: Materials in Electronics, 2021, 32, 3006-3018.	1.1	5
36	Vacancy-engineered MoO ₃ and Na ⁺ -preinserted MnO ₂ <i>in situ</i> grown N-doped graphene nanotubes as electrode materials for high-performance asymmetric supercapacitors. Journal of Materials Chemistry A, 2021, 9, 20794-20806.	5.2	15

#	Article	IF	CITATIONS
37	Self-templated induced carbon-supported hollow WS ₂ composite structure for high-performance sodium storage. Journal of Materials Chemistry A, 2021, 9, 21366-21378.	5.2	8
38	Controlled Synthesis of V-Doped Heterogeneous Ni ₃ S ₂ /NiS Nanorod Arrays as Efficient Hydrogen Evolution Electrocatalysts. Langmuir, 2021, 37, 357-365.	1.6	10
39	Enhanced Electrocatalytic Activity of Nickel Cobalt Phosphide Nanoparticles Anchored on Porous N-Doped Fullerene Nanorod for Efficient Overall Water Splitting. ACS Applied Materials & Interfaces, 2021, 13, 48949-48961.	4.0	37
40	Design Principles for Tungsten Oxide Electrocatalysts for Water Splitting. ChemElectroChem, 2021, 8, 4427-4440.	1.7	15
41	Synergy Strategy of Electrical Conductivity Enhancement and Vacancy Introduction for Improving the Performance of VS ₄ Magnesium-Ion Battery Cathode. ACS Applied Materials & Interfaces, 2021, 13, 54005-54017.	4.0	20
42	Heterostructured VN/Mo ₂ C Nanoparticles as Highly Efficient pH-Universal Electrocatalysts toward the Hydrogen Evolution Reaction. ACS Sustainable Chemistry and Engineering, 2021, 9, 15202-15211.	3.2	22
43	Fe ₂ P encapsulated in carbon nanowalls decorated with well-dispersed Fe ₃ C nanodots for efficient hydrogen evolution and oxygen reduction reactions. Nanoscale, 2021, 13, 17920-17928.	2.8	10
44	Co-Biodegradation of Naphthalene and Phenanthrene by <i>Acinetobacter johnsonii</i> . Polycyclic Aromatic Compounds, 2020, 40, 422-431.	1.4	9
45	Spatial-induced antiferromagnetic-like interaction of gadofullerene incarcerated in metal-organic-framework matrix. Fullerenes Nanotubes and Carbon Nanostructures, 2020, 28, 353-360.	1.0	2
46	Methanol-assisted synthesis of Ni ³⁺ -doped ultrathin NiZn-LDH nanomeshes for boosted alkaline water splitting. Dalton Transactions, 2020, 49, 1325-1333.	1.6	27
47	Carbon capsule confined Sb ₂ Se ₃ for fast Na ⁺ extraction in sodium-ion batteries. Sustainable Energy and Fuels, 2020, 4, 797-808.	2.5	12
48	Structure-controlled SnSe2 nanosheets as high performance anode material for lithium ion batteries. Ionics, 2020, 26, 2855-2862.	1.2	18
49	Rational Design of Coreâ€Shell Structured C@SnO ₂ @CNTs Composite with Enhanced Lithium Storage Performance. ChemElectroChem, 2020, 7, 1016-1022.	1.7	8
50	Enhanced visible-light photocatalytic activity of Ag/In2S3 photocatalysts induced by Schottky contact and SPR of Ag. Journal of Materials Science: Materials in Electronics, 2020, 31, 2089-2099.	1,1	10
51	Nitrogenâ€Ðoped Hard Carbon on Nickel Foam as Freeâ€Standing Anodes for Highâ€Performance Sodiumâ€lon Batteries. ChemElectroChem, 2020, 7, 604-613.	1.7	13
52	Controlled Growth of Edgeâ€Enriched ReS ₂ Nanoflowers on Carbon Cloth Using Chemical Vapor Deposition for Hydrogen Evolution. Advanced Materials Interfaces, 2020, 7, 2001196.	1.9	13
53	Graphene oxide and self-avoiding molecular recognition systems-assisted recombinase polymerase amplification coupled with lateral flow bioassay for nucleic acid detection. Mikrochimica Acta, 2020, 187, 667.	2.5	17
54	Controllable Conversion from Single-Crystal Nanorods to Polycrystalline Nanosheets of NiCoV-LTH for Oxygen Evolution Reaction at Large Current Density. ACS Sustainable Chemistry and Engineering, 2020, 8, 16091-16096.	3.2	25

#	Article	IF	CITATIONS
55	Spinel-Layered Intergrowth Composite Cathodes for Sodium-Ion Batteries. ACS Applied Materials & Interfaces, 2020, 12, 45997-46004.	4.0	26
56	Mo-Doped ultrafine VC nanoparticles confined in few-layer graphitic nanocarbon for improved electrocatalytic hydrogen evolution. Inorganic Chemistry Frontiers, 2020, 7, 4142-4149.	3.0	10
57	Densified Metallic MoS ₂ /Graphene Enabling Fast Potassiumâ€lon Storage with Superior Gravimetric and Volumetric Capacities. Advanced Functional Materials, 2020, 30, 2001484.	7.8	82
58	SnO2â^'x/Sb2O3 composites synthesized by mechanical milling method with excellent photocatalytic properties for isopropyl alcohol oxidation. Journal of Materials Science: Materials in Electronics, 2020, 31, 8564-8577.	1.1	3
59	Luminescent Properties of a Novel Blue-Emitting Mg2La8(SiO4)6O2:Ce3+ Phosphor with Apatite-Type Nanostructure. Journal of Nanoscience and Nanotechnology, 2020, 20, 2521-2525.	0.9	2
60	Layered-structure (NH ₄) ₂ Mo ₄ O ₁₃ @N-doped porous carbon composite as a superior anode for lithium-ion batteries. Chemical Communications, 2020, 56, 7757-7760.	2.2	7
61	Carbon microspheres coated with graphene oxide nanosheets as oil-based additives for tribological applications. Materials Today Communications, 2020, 25, 101271.	0.9	8
62	In Situ Construction of "Anchorâ€Like―Structures in FeNCN for Long Cyclic Life in Sodiumâ€Ion Batteries. Advanced Functional Materials, 2020, 30, 2000208.	7.8	19
63	In-situ optimizing the valence configuration of vanadium sites in NiV-LDH nanosheet arrays for enhanced hydrogen evolution reaction. Journal of Energy Chemistry, 2020, 47, 263-271.	7.1	66
64	The Sn–C bond at the interface of a Sn2Nb2O7–Super P nanocomposite for enhanced electrochemical performance. New Journal of Chemistry, 2020, 44, 4478-4485.	1.4	4
65	Synergistic effect of talc/carbon spheres composite as oilâ€based additive enhancing the lubricating properties for steelâ€steel contact. Lubrication Science, 2020, 32, 80-89.	0.9	14
66	Achieving excellent wide-range efficient microwave absorption property by synthesis of Fe-doped CuAlO2 powders via a facile sol–gel route. Journal of Materials Science: Materials in Electronics, 2020, 31, 9328-9334.	1.1	6
67	V-Doping Triggered Formation and Structural Evolution of Dendritic Ni ₃ S ₂ @NiO Core–Shell Nanoarrays for Accelerating Alkaline Water Splitting. ACS Sustainable Chemistry and Engineering, 2020, 8, 6222-6233.	3.2	66
68	Nanoporous NiAl-LDH nanosheet arrays with optimized Ni active sites for efficient electrocatalytic alkaline water splitting. Sustainable Energy and Fuels, 2020, 4, 2850-2858.	2.5	56
69	Confining FeS in graphitized carbon with void space for high and stable electrochemical storage performance of Na + and K +. International Journal of Energy Research, 2020, 44, 6595-6607.	2.2	6
70	Sulfurâ€doped shaddock peel–derived hard carbons for enhanced surface capacity and kinetics of lithiumâ€ion storage. International Journal of Energy Research, 2020, 44, 4026-4037.	2.2	10
71	Synthesis and tribological applications for carbon microspheres/poly (methyl methacrylate)/poly (ethylene imine) amphiphilic particles. Colloids and Surfaces A: Physicochemical and Engineering Aspects, 2020, 601, 124993.	2.3	5
72	Mg _{0.8} Zn _{0.2} O microspheres: preparation, characterization and application for degrading organic dyes. CrystEngComm, 2020, 22, 1273-1285.	1.3	6

#	Article	IF	CITATIONS
73	Turning waste makeup cotton to a hollow structured carbon as anode for highâ€performance lithium ions batteries. Micro and Nano Letters, 2020, 15, 1095-1098.	0.6	2
74	Tailoring MoS ₂ Ultrathin Sheets Anchored on Graphene Flexible Supports for Superstable Lithiumâ€lon Battery Anodes. Particle and Particle Systems Characterization, 2019, 36, 1900197.	1.2	7
75	Enhanced Kinetics over VS ₄ Microspheres with Multidimensional Na ⁺ Transfer Channels for Highâ€Rate Naâ€Ion Battery Anodes. ChemSusChem, 2019, 12, 5183-5191.	3.6	24
76	A Mini Review on Carbon Quantum Dots: Preparation, Properties, and Electrocatalytic Application. Frontiers in Chemistry, 2019, 7, 671.	1.8	366
77	O3â€Type Layered Niâ€Rich Oxide: A High apacity and Superiorâ€Rate Cathode for Sodiumâ€Ion Batteries. Si 2019, 15, e1905311.	nall, 5.2	41
78	Boosting the activity of Prussian-blue analogue as efficient electrocatalyst for water and urea oxidation. Scientific Reports, 2019, 9, 15965.	1.6	51
79	Carbon-Based Nanomaterials via Heterojunction Serving as Photocatalyst. Frontiers in Chemistry, 2019, 7, 713.	1.8	42
80	Label-Free Cross-Priming Amplification Coupled With Endonuclease Restriction and Nanoparticles-Based Biosensor for Simultaneous Detection of Nucleic Acids and Prevention of Carryover Contamination. Frontiers in Chemistry, 2019, 7, 322.	1.8	4
81	Co,N-Codoped porous vanadium nitride nanoplates as superior bifunctional electrocatalysts for hydrogen evolution and oxygen reduction reactions. Nanoscale, 2019, 11, 11542-11549.	2.8	53
82	MoO ₃ /Carbon Dots Composites for Liâ€lon Battery Anodes. ChemNanoMat, 2019, 5, 921-925.	1.5	25
83	Microscale flower-like magnesium oxide for highly efficient photocatalytic degradation of organic dyes in aqueous solution. RSC Advances, 2019, 9, 7338-7348.	1.7	81
84	Synthesis of Ag/Sm(OH)3 nanotubes with enhanced photocatalytic activity under visible light. Journal of Materials Science: Materials in Electronics, 2019, 30, 4370-4377.	1.1	3
85	Thin Carbon Layer Coated Porous Fe ₃ O ₄ Particles Supported by rGO Sheets for Improved Stable Sodium Storage. ChemistrySelect, 2019, 4, 2668-2675.	0.7	8
86	SnSe/r-GO Composite with Enhanced Pseudocapacitance as a High-Performance Anode for Li-Ion Batteries. ACS Sustainable Chemistry and Engineering, 2019, 7, 8637-8646.	3.2	55
87	Improved Li-Storage Properties of Cu ₂ V ₂ O ₇ Microflower by Constructing an in Situ CuO Coating. ACS Sustainable Chemistry and Engineering, 2019, 7, 6267-6274.	3.2	20
88	Bundled Defectâ€Rich MoS ₂ for a Highâ€Rate and Longâ€Life Sodiumâ€lon Battery: Achieving 3D Diffusion of Sodium Ion by Vacancies to Improve Kinetics. Small, 2019, 15, e1805405.	5.2	154
89	Simultaneous Nucleic Acids Detection and Elimination of Carryover Contamination With Nanoparticles-Based Biosensor- and Antarctic Thermal Sensitive Uracil-DNA-Glycosylase-Supplemented Polymerase Spiral Reaction. Frontiers in Bioengineering and Biotechnology, 2019, 7, 401.	2.0	2
90	A N/S-codoped disordered carbon with enlarged interlayer distance derived from cirsium setosum as high-performance anode for sodium ion batteries. Journal of Materials Science: Materials in Electronics, 2019, 30, 21323-21331.	1.1	2

#	Article	IF	CITATIONS
91	Sodiumâ€lon Batteries: O3â€Type Layered Niâ€Rich Oxide: A Highâ€Capacity and Superiorâ€Rate Cathode for Sodiumâ€lon Batteries (Small 52/2019). Small, 2019, 15, 1970282.	5.2	5
92	Synthesis and Tribological Performance of Carbon Microspheres/Poly(methyl methacrylate) Core–Shell Particles as Highly Efficient Lubricant. Journal of Physical Chemistry C, 2019, 123, 29037-29046.	1.5	13
93	Population pharmacokinetics and dosing optimization of latamoxef in neonates and young infants. International Journal of Antimicrobial Agents, 2019, 53, 347-351.	1.1	10
94	Controllable synthesis of 3D Urchin-like V2O5 as high-stability for Lithium-ion battery cathodes. Functional Materials Letters, 2019, 12, 1950037.	0.7	5
95	In Situ Topology Synthesis of Orthorhombic NaV ₂ O ₅ with High Pseudocapacitive Contribution for Lithium-Ion Battery Anode. ACS Sustainable Chemistry and Engineering, 2019, 7, 94-99.	3.2	8
96	Population Pharmacokinetics and Dosing Optimization of Amoxicillin in Neonates and Young Infants. Antimicrobial Agents and Chemotherapy, 2019, 63, .	1.4	29
97	Mutations of Mycobacterium tuberculosis induced by anti-tuberculosis treatment result in metabolism changes and elevation of ethambutol resistance. Infection, Genetics and Evolution, 2019, 72, 151-158.	1.0	10
98	Nitrogen-doped carbon-coated V2O5 nanocomposite as cathode materials for lithium-ion battery. Journal of Materials Science, 2018, 53, 10270-10279.	1.7	23
99	Facile synthesis of NH4V3O8 nanoflowers as advanced cathodes for high performance of lithium ion battery. Journal of Materials Science: Materials in Electronics, 2018, 29, 4830-4834.	1.1	2
100	Synthesis of Grainâ€like MoS ₂ for Highâ€Performance Sodiumâ€lon Batteries. ChemSusChem, 2018, 11, 2130-2137.	3.6	42
101	Effect of nano-SiO ₂ particles on the carbon fabric/resin friction materials by microwave-hydrothermal treatment. Journal of Composite Materials, 2018, 52, 245-252.	1.2	13
102	Controlling the Thickness of Disordered Turbostratic Nanodomains in Hard Carbon with Enhanced Sodium Storage Performance. Energy Technology, 2018, 6, 1080-1087.	1.8	25
103	<i>In situ</i> topotactic synthesis of a porous network Zn ₂ Ti ₃ O ₈ platelike nanoarchitecture and its long-term cycle performance for a LIB anode. CrystEngComm, 2018, 20, 7329-7336.	1.3	14
104	Novel Prussian-blue-analogue microcuboid assemblies and their derived catalytic performance for effective reduction of 4-nitrophenol. New Journal of Chemistry, 2018, 42, 20212-20218.	1.4	11
105	Tulip-like MoS ₂ with a single sheet tapered structure anchored on N-doped graphene substrates <i>via</i> C–O–Mo bonds for superior sodium storage. Journal of Materials Chemistry A, 2018, 6, 24433-24440.	5.2	48
106	Network Carbon with Macropores from Apple Pomace for Stable and High Areal Capacity of Sodium Storage. ACS Sustainable Chemistry and Engineering, 2018, 6, 14751-14758.	3.2	32
107	Influence and its mechanism of temperature variation in a muffle furnace during calcination on the adsorption performance of rod-like MgO to Congo red. Frontiers of Materials Science, 2018, 12, 304-321.	1.1	1
108	rs1800796 of the IL6 gene is associated with increased risk for anti-tuberculosis drug-induced hepatotoxicity in Chinese Han children. Tuberculosis, 2018, 111, 71-77.	0.8	7

#	Article	IF	CITATIONS
109	Well-dispersed ultrasmall VC nanoparticles embedded in N-doped carbon nanotubes as highly efficient electrocatalysts for hydrogen evolution reaction. Nanoscale, 2018, 10, 14272-14279.	2.8	58
110	Population Pharmacokinetics and Dosing Optimization of Azithromycin in Children with Community-Acquired Pneumonia. Antimicrobial Agents and Chemotherapy, 2018, 62, .	1.4	12
111	Sulfur nanodots as MoS ₂ antiblocking agent for stable sodium ion battery anodes. Journal of Materials Chemistry A, 2018, 6, 10535-10542.	5.2	48
112	Elemental Sulfur Nanoparticles Chemically Boost the Sodium Storage Performance of MoS ₂ /rGO Anodes. Batteries and Supercaps, 2018, 1, 184-191.	2.4	10
113	MoO ₂ @MoS ₂ Nanoarchitectures for High-Loading Advanced Lithium-Ion Battery Anodes. Particle and Particle Systems Characterization, 2017, 34, 1600223.	1.2	50
114	Efficient hydrogen evolution over Sb doped SnO2 photocatalyst sensitized by Eosin Y under visible light irradiation. Nano Energy, 2017, 36, 331-340.	8.2	168
115	Cf/C–SiC–MoSi2 composites with good ablation performance prepared via a two-step hydrothermal method. RSC Advances, 2017, 7, 11707-11718.	1.7	2
116	Adjusting the Chemical Bonding of SnO ₂ @CNT Composite for Enhanced Conversion Reaction Kinetics. Small, 2017, 13, 1700656.	5.2	111
117	Discovery of susceptibility loci associated with tuberculosis in Han Chinese. Human Molecular Genetics, 2017, 26, 4752-4763.	1.4	50
118	Facile in situ synthesis of crystalline VOOH-coated VS ₂ microflowers with superior sodium storage performance. Journal of Materials Chemistry A, 2017, 5, 20217-20227.	5.2	74
119	Electromagnetic wave absorption properties of a carbon nanotube modified by a tetrapyridinoporphyrazine interface layer. Journal of Materials Chemistry C, 2017, 5, 7479-7488.	2.7	146
120	Manganese dioxide nanoflakes anchored on reduced graphene oxide with superior electrochemical performance for supercapacitors. Micro and Nano Letters, 2017, 12, 147-150.	0.6	2
121	Influences of acid and heat treatments on the structure and water vapor adsorption property of natural zeolite. Surface and Interface Analysis, 2017, 49, 1249-1255.	0.8	28
122	Shape Evolution of Hierarchical W18O49 Nanostructures: A Systematic Investigation of the Growth Mechanism, Properties and Morphology-Dependent Photocatalytic Activities. Nanomaterials, 2016, 6, 240.	1.9	13
123	Synthesis of Structurally Stable 3D MoS ₂ Architectures as High Performance Lithiumâ€ion Battery Anodes. Particle and Particle Systems Characterization, 2016, 33, 311-315.	1.2	14
124	Influence of hydrothermal treatment on the microstructure and oxidation resistance of a Zn4B2O7·H2O (4ZnO·B2O3·H2O) coating for C/C composites. Materials at High Temperatures, 2016, 33, 283-287.	0.5	1
125	High Pseudocapacitance in FeOOH/rGO Composites with Superior Performance for High Rate Anode in Li-Ion Battery. ACS Applied Materials & Interfaces, 2016, 8, 35253-35263.	4.0	119
126	Rs1914663 of SFTPA 1 gene is associated with pediatric tuberculosis in Han Chinese population. Infection, Genetics and Evolution, 2016, 41, 16-20.	1.0	2

#	Article	IF	CITATIONS
127	Hydrothermal Synthesis and Electrochemical Property of Self-Assembly K ₁₀ [H ₂ W ₁₂ O ₄₂]â<10H ₂ O Nanorod. Nano, 2016, 11, 1650062.	0.5	0
128	Soft chemical in situ synthesis and photocatalytic performance of 1D Ag/AgCl/V2O5 hetero-nanostructures. Materials Letters, 2016, 183, 215-218.	1.3	9
129	Utility of Novel Plasma Metabolic Markers in the Diagnosis of Pediatric Tuberculosis: A Classification and Regression Tree Analysis Approach. Journal of Proteome Research, 2016, 15, 3118-3125.	1.8	20
130	Improved Na Storage Performance with the Involvement of Nitrogen-Doped Conductive Carbon into WS ₂ Nanosheets. ACS Applied Materials & Interfaces, 2016, 8, 23899-23908.	4.0	65
131	Enhanced Performance by Enlarged Nano-pores of Holly Leaf-derived Lamellar Carbon for Sodium-ion Battery Anode. Scientific Reports, 2016, 6, 26246.	1.6	33
132	pH-regulated template-free assembly of Sb4O5Cl2 hollow microsphere crystallites with self-narrowed bandgap and optimized photocatalytic performance. Scientific Reports, 2016, 6, 27765.	1.6	30
133	Ti-O-O coordination bond caused visible light photocatalytic property of layered titanium oxide. Scientific Reports, 2016, 6, 29049.	1.6	50
134	Identification of differentially expressed transcripts targeted by the knockdown of endogenous IFITM3. Molecular Medicine Reports, 2016, 14, 4367-4373.	1.1	7
135	Comparative study on the photocatalytic activity of biomass carbon doped Bi2WO6 crystallite with self-assembled hierarchical structure. Journal of Materials Science: Materials in Electronics, 2016, 27, 2473-2480.	1.1	8
136	In situ synthesis and photocatalytic performance of WO ₃ /ZnWO ₄ composite powders. RSC Advances, 2016, 6, 23783-23789.	1.7	16
137	Tailoring MoO ₂ /Graphene Oxide Nanostructures for Stable, Highâ€Density Sodiumâ€lon Battery Anodes. Energy Technology, 2015, 3, 1108-1114.	1.8	59
138	V ₂ O ₅ nanoflowers assembled by nanorods as cathode material for lithiumâ€ion batteries. Micro and Nano Letters, 2015, 10, 686-688.	0.6	5
139	Preparation and characterization of natural zeolite supported nano TiO ₂ photocatalysts by a modified electrostatic self-assembly method. Surface and Interface Analysis, 2015, 47, 142-147.	0.8	11
140	Toll-like receptor 1(TLR1) Gene SNP rs5743618 is associated with increased risk for tuberculosis in Han Chinese children. Tuberculosis, 2015, 95, 197-203.	0.8	33
141	One-step synthesis of C–Bi ₂ WO ₆ crystallites with improved photo-catalytic activities under visible light irradiation. RSC Advances, 2015, 5, 66464-66470.	1.7	12
142	Soft chemical in situ synthesis, formation mechanism and electrochemical performances of 1D bead-like AgVO ₃ nanoarchitectures. Journal of Materials Chemistry A, 2015, 3, 18127-18135.	5.2	25
143	Effects of NBR Particle Size on Performance of Carbon Fiber–Reinforced Paper-Based Friction Material. Tribology Transactions, 2015, 58, 1012-1020.	1.1	13
144	Controllable synthesis and morphology evolution from two-dimensions to one-dimension of layered K ₂ V ₆ O ₁₆ ·nH ₂ O. CrystEngComm, 2015, 17, 3777-3782.	1.3	11

#	Article	IF	CITATIONS
145	Li4Ti5O12 hollow mesoporous microspheres assembled from nanoparticles for high rate lithium-ion battery anodes. RSC Advances, 2015, 5, 35643-35650.	1.7	19
146	Sweet potato-derived carbon nanoparticles as anode for lithium ion battery. RSC Advances, 2015, 5, 40737-40741.	1.7	70
147	Effect of hydrothermal modified carbon fiber through Diels–Alder reaction and its reinforced phenolic composites. RSC Advances, 2015, 5, 64450-64455.	1.7	13
148	Performance of the Interferon Gamma Release Assays in Tuberculosis Disease in Children Five Years Old or Less. PLoS ONE, 2015, 10, e0143820.	1.1	16
149	A 3'UTR Polymorphism of IL-6R Is Associated with Chinese Pediatric Tuberculosis. BioMed Research International, 2014, 2014, 1-7.	0.9	5
150	Topotactic synthesis and photocatalytic performance of one-dimensional ZnNb ₂ O ₆ nanostructures and one-dimensional ZnNb ₂ O ₆ /KNbO ₃ hetero-nanostructures. RSC Advances, 2014, 4, 56637-56644.	1.7	14
151	Topotactic soft chemical synthesis and photocatalytic performance of one-dimensional AgNbO3 nanostructures. Materials Letters, 2014, 137, 110-112.	1.3	14
152	rs2243268 and rs2243274 of Interleukin-4 (IL-4) gene are associated with reduced risk for extrapulmonary and severe tuberculosis in Chinese Han children. Infection, Genetics and Evolution, 2014, 23, 121-128.	1.0	14
153	Genetic Contribution of CISH Promoter Polymorphisms to Susceptibility to Tuberculosis in Chinese Children. PLoS ONE, 2014, 9, e92020.	1.1	17
154	Impact of Glutathione S-Transferase M1 and T1 on Anti-Tuberculosis Drug–Induced Hepatotoxicity in Chinese Pediatric Patients. PLoS ONE, 2014, 9, e115410.	1.1	17
155	Influence of ethanol on the HAp coatings prepared by hydrothermal electrodeposition on C/C composites. Journal of Coatings Technology Research, 2010, 7, 67-71.	1.2	10
156	New Energy Balance Controller of Thermal Generating Unit. , 2010, , .		0
157	Structure and oxidation behavior of a plasma sprayed yttrium silicates coated SiC-C/C with a glass outer sealant from 1 573K to 1 873K. Journal Wuhan University of Technology, Materials Science Edition, 2008, 23, 33-37.	0.4	4
158	Ni(OH)2 Nanosheets Modified Hexagonal Pyramid CdS Formed Type II Heterojunction Photocatalyst with High-Visible-Light H2 Evolution. ACS Applied Energy Materials, 0, , .	2.5	12
159	Equal contents of intrinsic defects and oxygen-containing defects promote carbon electrodes to achieve high sulfur loads. Journal of Nanostructure in Chemistry, 0, , 1.	5.3	2
160	Fullerene nanorods supported cobalt nickel sulfide composite as efficient electrocatalyst for oxygen evolution. Fullerenes Nanotubes and Carbon Nanostructures, 0, , 1-7.	1.0	1